

# TerEffic: Highly Efficient Ternary LLM Inference on FPGA

Chenyang Yin\*, Zhenyu Bai†, Pranav Venkatram†, Shivam Aggarwal†, Zhaoying Li†, and Tulika Mitra†

\*School of Electronic Engineering and Computer Science, Peking University

Email: ycy@stu.pku.edu.cn

†School of Computing, National University of Singapore

Email: zhenyu.bai@nus.edu.sg

Email: e0552200@u.nus.edu

Email: shivam@comp.nus.edu.sg

Email: zhaoying@comp.nus.edu.sg

Email: tulika@comp.nus.edu.sg

**Abstract**—Large Language Model (LLM) deployment on edge devices is typically constrained by the need for off-chip memory access, leading to high power consumption and limited throughput. Ternary quantization for LLMs is promising in maintaining model accuracy while reducing memory footprint. However, existing accelerators have not exploited this potential for on-chip inference. We present TerEffic, an FPGA-based accelerator that carefully co-designs memory architecture and computational units to unlock highly efficient LLM inference with fully on-chip execution. Through weight compression, custom computational units, and memory hierarchy optimization, we achieve unprecedented efficiency by eliminating off-chip memory bandwidth bottlenecks. We propose two architectural variants: a fully on-chip design for smaller models and an HBM-assisted design for larger ones. When evaluated on a 370M parameter model with single-batch inference, our on-chip design achieves 12,700 tokens/sec (149× higher than NVIDIA’s Jetson Orin Nano) with a power efficiency of 467 tokens/sec/W (19× better than Jetson Orin Nano). The HBM-assisted design provides 521 tokens/sec on a 2.7B parameter model (2× higher than NVIDIA’s A100) with 33W power consumption, achieving a power efficiency of 16 tokens/sec/W (8× better than A100).

**Index Terms**—Architecture, FPGA, AI, LLM.

## I. INTRODUCTION

Large Language Models (LLMs) have revolutionized AI with breakthrough capabilities. While state-of-the-art LLMs like ChatGPT [1], Claude [2], and Google Gemini [3] have hundreds of billions of parameters, a significant trend has emerged toward creating smaller yet highly capable models through advanced techniques like knowledge distillation [4]. For instance, Meta’s Llama3.2 [5] includes lightweight 1B and 3B models for high-performance edge applications like text generation. Similarly, GPT-4o mini [6] exceeds GPT-4’s capabilities while reducing inference costs by 60% compared to GPT-3.5 Turbo, and it is believed to be comparable in scale to Llama3-8B model [7].

Most existing AI inference accelerators, such as GPUs, rely on off-chip DRAM due to limited on-chip memory capacity. However, accessing off-chip DRAM or HBM is less power-efficient and scaling the memory bandwidth suffers from the *memory wall* [8] problem. As shown in Figure 1, an increase in model parameters results in decreased inference

throughput and greater energy consumption. Although on-chip memory offers significantly better power efficiency and higher throughput, its limited capacity hinders large model acceleration. However, the prevailing trend to develop smaller models reduces memory capacity requirements, allowing an entire model’s weights to fit within on-chip memory, thereby improving overall system efficiency. Quantization techniques further reduce memory requirements [9]–[15] wherein activations and/or weights are represented using reduced-precision data types. For example, binary and ternary quantizations represent weights using just two values {-1, 1} or three values {-1, 0, 1}, respectively. Since a binary or ternary weight can be stored using less than 2 bits, such LLMs are known as ‘1-bit’ LLMs. Despite low-precision weights, 1-bit LLMs have the potential to achieve similar accuracy of full-precision models [14]–[18]. Low-bit quantizations open the door to fully on-chip inference for larger models at substantially higher throughput and lower energy as shown in Figure 1. However, existing hardware, such as CPUs and GPUs, lacks the architectural support to unlock the potential of low-bit quantizations, underscoring the need for specialized hardware designs.

To address this gap, we propose **TerEffic**, a custom architecture on FPGA to fully unlock the potential of on-chip inference. We focus on ternary quantization due to its superior accuracy compared to binary approaches [14], [15]. Our design encompasses three key innovations: a **1.6-Bit Weight Compression** method that approaches the theoretical minimum of 1.58 bits per weight, a custom **Ternary MatMul Unit (TMU)** optimized for ternary computations, and a **Compute-Memory Alignment** strategy that maximizes the utilization of on-chip memory bandwidth and capacity. We propose two architectural variants. Our **fully on-chip architecture** supports models of up to 1.3B parameters. For a 370M parameter model with single-batch inference, our design achieves a throughput of 12,700 tokens/sec (149× higher) and a power efficiency of 467 tokens/sec/W (19× better) compared to NVIDIA’s Jetson Orin Nano. For multi-batch inference, our approach leverages **pipeline parallelism**, yielding a 130,200

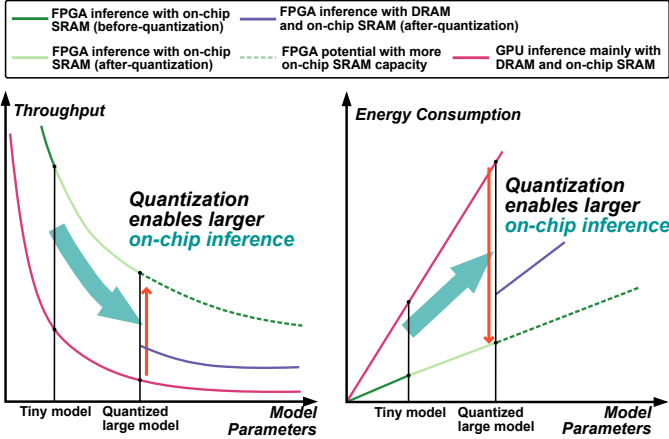


Fig. 1: On-Chip vs. off-chip memory for inference: Throughput and energy trends with increasing model parameters

tokens/sec throughput ( $119\times$  higher) and a 2,770 tokens/sec/W power efficiency ( $12\times$  better). For larger models that exceed the on-chip memory capacity, we propose an **HBM-assisted architecture** that maintains high performance through **full-resource parallelism**, minimizing the impact of off-chip memory access.

## II. BACKGROUND & RELATED WORK

### A. Binary and Ternary Quantizations

Quantization is a key strategy to accelerate inference as neural networks grow rapidly in parameter count. Binary and Ternary quantization were initially validated in CNN models such as BNN [19], XNOR-Net [20], and TWN [21], achieving high efficiency with minimal accuracy loss.

In the era of LLMs, large model sizes and limited hardware resources necessitate low-precision quantization, especially in the context of edge devices. As a pioneer, BitNet [14] employed binary quantization and introduced BitLinear as a replacement for matrix multiplications (MatMuls) in linear projections. As its variant and improvement, BitNet 1.58b [15] matched the performance of full-precision (fp16 or bf16) transformers using ternary quantization. Furthermore, the 1-bit model was extended to the Vision Transformer (ViT) domain [17] and a scaling law [18] was established, providing a theoretical basis for the impressive performance of these models. Advances in post-training reparameterization [22] also paved the way for low-cost training of 1-bit LLMs.

### B. FPGA-based Transformer Accelerators

Field-programmable gate arrays (FPGAs) are widely used for accelerating various tasks.

In the context of deep learning, several works have contributed toward accelerating transformer inference using FPGAs. FTRANs [23] was the earliest accelerator specifically designed for Transformers featuring an enhanced block-circulant matrix-based weight representation. The NPE [24] flexible overlay processor offered a common method for approximating different nonlinear functions. The HPTA [25] accelerator provided support for several transformer variants without

needing FPGA reconfiguration. DFX [26] presented an end-to-end design for Generative Pretrained Transformer (GPT) model inference. [27] proposed efficient algorithm–hardware co-designs with sparse attention and dynamic pipelining. [28] built an HLS kernel library for FPGA-based LLM spatial acceleration. FlightLLM [29] introduced a sparse DSP chain to support different sparsity patterns and an always-on-chip decode scheme to reduce memory overhead. EdgeLLM [30] proposed a CPU-FPGA heterogeneous acceleration system with a unified and universal data format and customized FP16\*INT4 computational units.

So far, on-chip inference on FPGA has been minimally explored, yet 1-bit quantization offers a promising avenue for this efficient paradigm. FPGAs provide an ideal platform to harness the advantages of 1-bit LLMs, thanks to their bit-level reconfigurability that enables customized memory architectures and computational units. While [16] proposed a basic FPGA implementation for their ternary model, their prototype lacked effective hardware optimizations and failed to leverage the on-chip potential.

## III. TEREFFIC KEY INNOVATIONS

To enable efficient on-chip inference of ternary LLMs, we introduce three key innovations:

- 1) **1.6-Bit Weight Compression:** Our method encodes ternary weights  $\{-1, 0, 1\}$  using only 1.6 bits per weight, approaching the theoretical minimum of 1.58 bits. This 20% reduction in memory footprint compared to 2-bit encoding enables larger models to fit on-chip.
- 2) **Ternary MatMul Unit (TMU):** We optimize ternary matrix multiplications (MatMuls) through specialized hardware units that reduce complex operations such as negation and leverage FPGA-native multiplexers. This customization reduces Look-up Table (LUT) usage by 40% while maintaining high computational throughput.
- 3) **Compute-Memory Alignment:** Our hybrid URAM-BRAM memory architecture balances computational power, memory bandwidth, and capacity. By storing weights in URAM and intermediate values in BRAM, we achieve optimal resource utilization without bandwidth bottlenecks or wasted resources.

### A. 1.6-Bit Weight Compression

To encode ternary weights  $\{-1, 0, 1\}$  with binary bits, the theoretical lower bound is 1.58 bits [15]. However, achieving exactly 1.58 bits is not feasible in hardware, while a straightforward 2-bit representation introduces 25% redundancy. To overcome this challenge, we adapt and optimize the encoding scheme from [31] to create an efficient 1.6-bit compression method that closely approaches the theoretical limit while remaining hardware-friendly.

We observe that 5 ternary weights have 243 possible combinations whereas 8 binary bits can represent 256 distinct values. Hence, we encode 5 ternary weights using 8 bits, averaging 1.6 bits per weight. The encoding and decoding scheme is shown in Fig. 2. For example, five original weights  $\{-1, 0, 0, 1, 1\}$

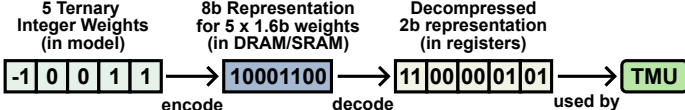


Fig. 2: 1.6-Bit Weight Compression

are encoded into 8 bits (10001100) when stored in memory. During inference, the 8-bit encoded weight is decoded into five 2-bit representations, where 01 corresponds to 1, 11 to -1, and 00 to 0. As the decoding involves only bitwise operations, such as + and &, it incurs minimal hardware cost and latency. This method can store and transfer 25% more data compared to the regular 2-bit representation, effectively improving throughput and energy efficiency.

### B. Ternary MatMul Unit

MatMuls account for the largest portion (65%-85%) of the computational workload [32] in typical LLMs. To achieve the full potential of ternary LLMs, we replace costly MatMuls with optimized **Ternary MatMuls Units (TMUs)** that are much cheaper.

A naive TMU design is shown in Fig. 3a. Here, the partial sum ( $S$ ) is either added or subtracted by the activation ( $X$ ), or remains unchanged depending on the weight ( $W \in \{1, -1, 0\}$ ). We identify inefficiencies in this simple design and propose the corresponding optimizations. First, the activation ( $X$ ) is broadcast to multiple TMUs in parallel (as elaborated in Section IV.A). Therefore, performing complex operations, such as negation, within each TMU harms efficiency. To address this, we pre-calculate the negation outside the TMUs, providing both the activation and its negation as TMU inputs. Secondly, as the default logic units, LUTs cannot directly implement conditional statements but decompose them into a series of mapping relations. This indirect mapping causes resource wastage. We resolve this by leveraging another basic FPGA resource, the 2-to-1 multiplexer (Mux), specialized for the selection logic. With each weight decoded to 2 bits (as presented in Section III-A), the high bit ( $W[1]$ ) serves as the select signal for the Mux, while the low bit ( $W[0]$ ) determines whether the Mux's output should be retained or transformed into zero. By integrating the two optimizations, we introduce an improved TMU design illustrated in Fig. 3b, which achieves approximately 40% LUT savings for the whole design.

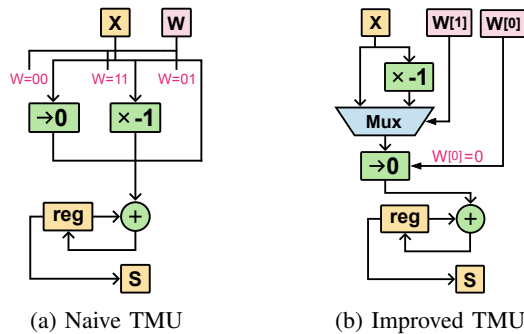


Fig. 3: Improvements in the TMU Design

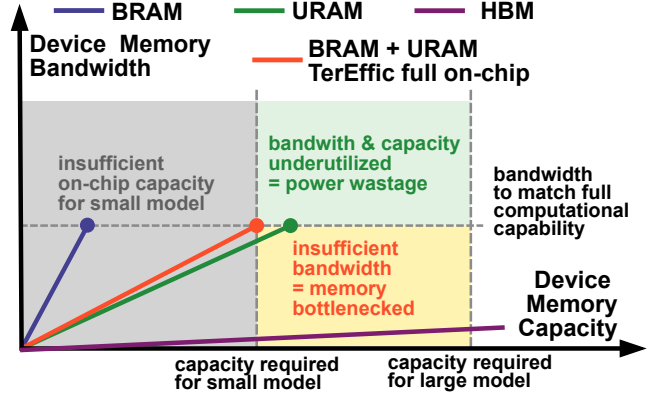


Fig. 4: Compute-Memory Alignment

### C. Compute-Memory Alignment

Xilinx U280 FPGA offers two types of on-chip SRAM: BlockRAM (BRAM) and UltraRAM (URAM), as shown in Table I. To align with the substantial computational capability offered by TMU, an intricate memory architecture is required to provide enough bandwidth while avoiding excessive bandwidth which will cause power wastage. At the same time, the memory architecture must offer sufficient capacity for on-chip weight storage while optimizing memory capacity utilization to minimize power wastage.

TABLE I: Attributes of On-chip BRAM and URAM on U280

SRAM	Capacity/piece	Bandwidth/piece	Number	Total Capacity
BRAM	36Kb	72b	2,016	8.85MB
URAM	288Kb	144b	960	33.75MB

Fig. 4 illustrates memory choices where each point depicts the bandwidth and capacity provided by a certain memory architecture. The horizontal dotted line represents the required bandwidth to align with the maximum computational capability of the device, while the vertical dotted lines indicate the required memory capacity that increases with the model size. As shown by the blue line, a fully BRAM-based architecture lacks sufficient memory capacity. Conversely, a fully URAM-based architecture (the green line) suffers from low bandwidth, also resulting in power wastage.

Therefore, we propose a **hybrid fully on-chip architecture** (the orange line) storing weights in URAM and buffering intermediate values in BRAM. Our design falls approximately on the intersection of the dotted lines in Fig. 4, enabling full utilization of computational power, memory bandwidth, and capacity concurrently. However, it can be observed that as the model size increases, the on-chip memory capacity will eventually fail to meet the storage requirements. In such cases, the large capacity of off-chip HBM is still required, while its limited bandwidth bottlenecks the performance (shown in the purple line). To alleviate this issue, we introduce an **HBM-assisted architecture** with effective parallelization, proposed in Section IV-B2.

## IV. TEREFFIC ARCHITECTURE DESIGN

We design a ternary LLM accelerator architecture on FPGA to showcase the benefits of the aforementioned optimizations. We choose the MatMul-free LM model [16] as the representative ternary LLM for our design. Although [16] also proposed

an FPGA design, it was a simple and inefficient prototype as their main focus was on the model architecture.

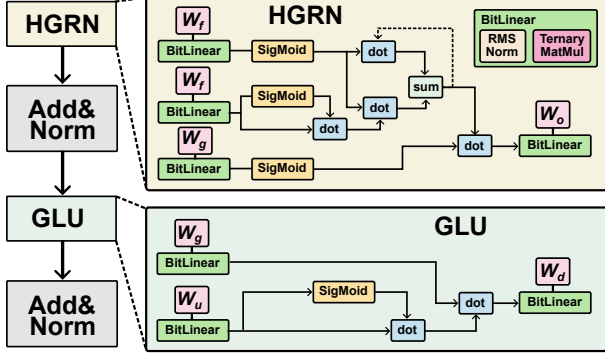


Fig. 5: TerEffic Hardware Architecture

#### A. Architecture Overview

TerEffic overall hardware architecture is shown in Fig.5, along with its two major components, the HGRN [33] and the GLU [34] module. HGRN is a powerful RNN-based alternative to the self-attention mechanism [35], while GLU, widely utilized in models like Llama [36], serves as a robust enhancement for feed-forward networks (FFNs). In the model, addition, subtraction, and dot product (Dot) can be directly implemented using LUTs and DSPs, while the sigmoid function is approximated by piecewise linear equations [37]. Consequently, the primary implementation challenge lies in the BitLinear module consisting of a Root-Mean-Square Normalization (RMSNorm) module and a ternary MatMul module.

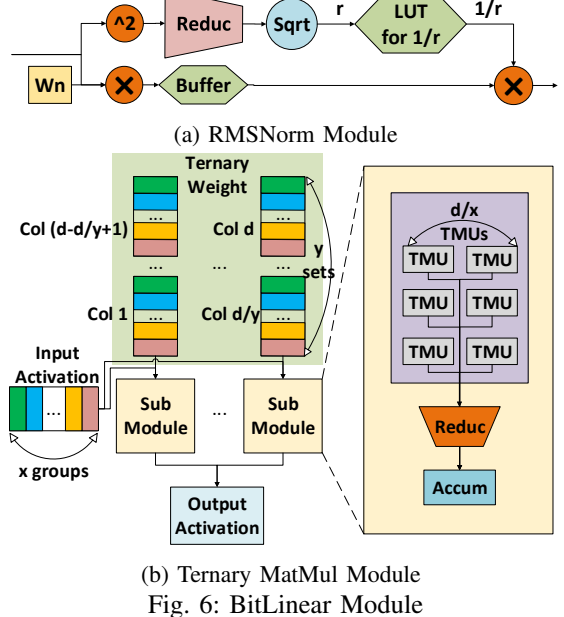
1) *RMSNorm module*: The RMSNorm [38] is more computationally efficient than the traditional LayerNorm [35] but maintains high accuracy, making it well-suited for FPGA. The algorithm for RMSNorm is presented below:

$$r = \sqrt{\frac{1}{d} \sum_{i=1}^d x_i^2 + \epsilon} \quad , \quad \text{RMSNorm}(X) = \frac{X \odot W_n}{r} \quad (1)$$

where  $X \in \mathbb{R}^{1 \times d}$  denotes the input activation,  $W_n \in \mathbb{R}^{1 \times d}$  denotes the normalization weight,  $r$  denotes the RMS result and  $\epsilon$  is a small constant. As shown in the architecture in Fig. 6a, the computation of  $r$  and  $X \odot W_n$  can be executed in parallel. As the former has longer latency, the results of  $X \odot W_n$  are temporarily stored in on-chip buffers. These results are then repeatedly retrieved from the buffers to match the multiple iterations required by the subsequent ternary MatMul modules. Moreover, as divisions incur high hardware cost and long cycle latency, we replace the divisions ( $\div r$ ) with DSP-based multiplications ( $\times \frac{1}{r}$ ), using  $r$  as an index to retrieve  $1/r$  from an on-chip look-up table consisting of a small amount of SRAM. This method saves hardware resources and significantly increases maximum frequency.

2) *Ternary MatMul Module*: The Ternary MatMul Module serves as the primary computational core executing  $X \times W$ , where  $X \in \mathbb{R}^{1 \times d}$  denotes the normalized activation and  $W \in \mathbb{R}^{d \times d}$  denotes the ternary weight matrix. The module consists of submodules that perform the dot product between  $X$  and one column of  $W$ . Each submodule is made up of TMUs for

ternary MatMuls and a reduction tree to aggregate the TMU outputs. A detailed architecture is shown in Fig.6b. To address the memory bandwidth limitations, we partition  $X$  and each column of  $W$  into  $x$  groups. Each submodule, which contains  $\frac{d}{x}$  TMUs, computes the MatMuls for one group. Moreover, due to the limited computational capacity, the  $d$  columns of  $W$  are divided into  $y$  sets and processed sequentially by  $\frac{d}{y}$  submodules. The values of  $x$  and  $y$  are set based on the on-chip memory bandwidth and computing capacity, optimized by the alignment strategy discussed in Section III-C.



(a) RMSNorm Module

(b) Ternary MatMul Module

Fig. 6: BitLinear Module

#### B. Architecture Variants

We propose two memory architectures—one aims to store all weights in on-chip memory, and another utilizes an HBM. Since a single card is insufficient to hold all the weights of a moderate-sized model, the fully-on-chip architecture may need to leverage multiple cards. For larger models, we switch to HBM-assisted architecture that requires only one card for weight storage. We explore different parallelism methods in both architectures to achieve higher energy efficiency. Though the methods differ from the batching method for GPU, we use terms like 'multi-batch' and 'batch size' for convenience.

1) *TerEffic On-Chip Architecture*: The on-chip architecture corresponds to the orange line in Fig. 4, where we store all weights on-chip and benefit from the massive on-chip bandwidth. The basic design is based on the 24-layer, 370M model from [16]. Each layer is segmented into 10 main stages, as shown in Fig. 7 (Norm denotes RMSNorm and TMM denotes ternary MatMul), with the latency of each stage indicated in the red row. Through the optimizations discussed before, the latency per layer is 820 cycles, resulting in a total latency of  $\approx 20,000$  cycles across all 24 layers.

After 1.6-Bit Weight Compression, the 370M model occupies  $\approx 57.6\text{MB}$  of memory, exceeding the on-chip capacity of 42MB (see TABLE I). Thus, a 2-card system is required, with each card holding the weights for 12 layers and processing them accordingly, as shown in Fig. 8a. As the model size

Stages in 1 layer	HGRN				GLU				Overall Latency		
	Norm	TMM	Norm	TMM	Add&Norm	Norm	TMM	Norm	TMM	Add&Norm	
Single Batch Pipeline	29	160	29	160	29	29	160	29	160	29	~820
Pipeline	160	160	160	160	160	160	160	160	160	160	1600
Full-Resource	29	480	29	160	29	29	853	29	427	29	~2600

Fig. 7: Stage latency of a layer for on-chip single-batch, on-chip multi-batch (with pipeline parallelism), and HBM-assisted multi-batch (with full-resource parallelism)

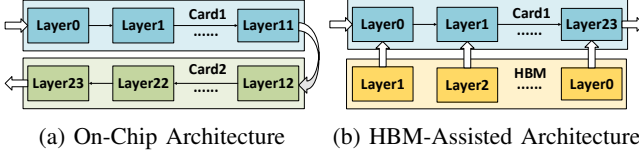


Fig. 8: TerEffic Architecture Variants

increases, more cards become necessary—for instance, the 1.3B model requires eight cards each storing three layers.

Though this design delivers the shortest latency, the power efficiency is relatively low as only a portion of the resources is utilized at any point in time. To better harness parallelism, we construct a **pipeline**. A simple 2-stage example is illustrated in Fig. 9a, where a batch size of two is processed concurrently by different TMUs. As shown by the purple row in Fig. 7, each pipeline stage takes 160 cycles, resulting in a single-layer latency of 1600 cycles. With each card handling up to a batch size of 10, the 2-card system can process a batch size of 20, boosting throughput by 10× over the basic design.

2) *TerEffic HBM-Assisted Architecture*: For larger models, an HBM-assisted architecture (Fig. 8b) is required. Xilinx U280 FPGA features 8GB HBM with 32 channels, providing a total maximum bandwidth of 8Kb. As discussed in Section III-C, the HBM’s bandwidth is much lower than on-chip memory, resulting in a longer latency of about 2,400 cycles/layer.

For this architecture, the pipeline parallelism is not suitable, as the latency after pipelining is shorter than the data-fetch latency from HBM. Moreover, pipelining requires two layers of weights stored on-chip in a ping-pong buffer, which is infeasible for large models. Hence, we introduce **full-resource parallelism** with a simplified example (2 stages, batch size=2) presented in Fig. 9. Unlike in the previous pipeline, all the TMUs are utilized for processing each stage. As the batch size increases, the TMUs available for each input decrease and the latency increases. We set the batch size to 15 to accommodate 2,400 cycle HBM data-fetch latency. The detailed latency is shown in the orange row in Fig. 7, where the latency of each TMM stage is proportional to the computational workload.

## V. EVALUATION

### A. Evaluation Methodology

We implement both our architectures on Xilinx Alveo U280 FPGA. We use the ternary-quantized models from [16] for inference performance evaluation. We first compare our performance and power consumption against a simplistic FPGA implementation of the ternary model [16] to show the benefits of our architectural designs. That basic design adopts a CPU-like architecture that only supports single-batch tasks while

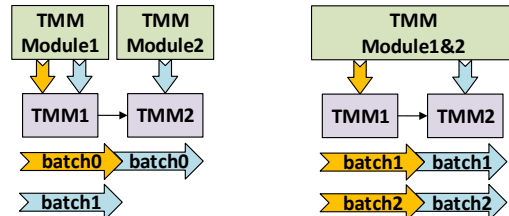


Fig. 9: Parallelism Methods

using off-chip memory to store the weights, which leads to a memory-bottlenecked implementation.

TABLE II: Attributes of the Evaluation Models

Parameter	Dimension	Layer	Storage Size
370M	1K	24	58MB
1.3B	2K	24	230MB
2.7B	2.5K	32	480MB

To further highlight the performance of our design, we deploy the GPU baselines with the 370M model on NVIDIA Jetson Orin Nano, using TensorRT [39] to maximize GPU performance. As the 1.3B and 2.7B models cannot fit into Jetson Orin Nano, we conduct experiments on NVIDIA’s A100 GPU with TensorRT. The models are quantized to the lowest supported precision for GPU deployment: INT8 for the Jetson Orin Nano and INT4 for the A100. While the model precisions on the GPUs differ from our ternary design, [16] demonstrated that the models maintain high performance under ternary quantization. Although *TerEffic* only accelerates the transformer blocks, our experiments show that the excluded layers (embedding layer, position encoding, and output layer) account for less than 0.1% of the total GPU inference time, making the throughput comparison reasonable.

### B. FPGA Resource Utilization

We perform synthesis on Vivado v2022.1 and achieve **250MHz** frequency. The resource utilization of the On-Chip Architecture is presented in Table III, while the HBM-Assisted version is the same except for the inclusion of HBM.

TABLE III: *TerEffic* FPGA Resource Utilization

LUT	Reg	Carry8	Mux	DSP	BRAM	URAM
862K	700K	82K	542K	1,551	385.5	865
66.12%	26.88%	50.13%	83.03%	17.19%	19.12%	90.10%

As our FPGA design adopts customized TMUs made up of LUTs and Muxes, their utilizations are significantly higher than that of costly DSPs. Moreover, as discussed in Section III-C, we choose URAM to store weights instead of BRAM, which accounts for the high URAM utilization and low BRAM utilization.

### C. On-Chip Architecture Evaluation

The single-batch latency of the on-chip architecture for the 370M model is  $820 \times 24$  layers = 19680 cycles, leading to a single-batch throughput of **~12,700 tokens/sec**. With **pipeline parallelism**, the maximum batch size for the 2-card system is 20 and the multi-batch throughput is thereby **~130,200 tokens/sec**. As only activations are transmitted between the two cards, the inter-card communication overhead is negligible and not included.

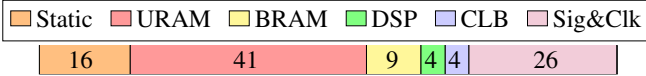


Fig. 10: FPGA Power Breakdown (%) for the on-chip design

We estimate power for one card using Vivado as  $P_0 = 23.5\text{W}$ . A detailed power breakdown is shown in Fig. 10, where CLB contains LUT, Regs, muxes and other logic, and Sig&Clk denotes signals and clock. The majority of power consumption originates from the URAM due to frequent weight transfer, underscoring the importance of our hybrid memory architecture. Moreover, CLB consumes little power (4%) despite handling most of the computational workload, emphasizing the high efficiency of the TMUs.

When the 2-card system is executing a single-batch task, only one card is active, while the other remains idle and only consumes 3.7W static power ( $P_{\text{static}}$ ). Therefore, the overall power estimation is  $P_0 + P_{\text{static}} = 27.2\text{W}$ . In contrast, when running multi-batch tasks, the inputs are executed in a pipeline manner and all cards contribute to full power consumption, leading to  $P = 2 \times P_0 = 47.0\text{W}$ .

TABLE IV: Comparison of *TerEffic* (On-Chip) with GPU and a simplistic FPGA design [16] for a 370M model.

Hardware	Batch Size	TP (tk/s)	TP Impv	Power (W)	Eff (tk/s/W)	Eff Impv
FPGA [16]	1	62	0.7×	13.7	5	0.2×
Jetson	1	85	1×	3.5	24	1×
<i>TerEffic</i>	1	12,700	149×	27.2	467	19×
Jetson	20	1,096	1×	4.6	240	1×
<i>TerEffic</i>	20	130,200	119×	47.0	2,770	12×

We compare our on-chip results on the 370M model with the FPGA results from [16] and the experimental results on Jetson Orin Nano, with the GPU batch size set to 1 and 20 to match our design (see Section IV-B1). The comparison is presented in TABLE IV, where TP denotes throughput (tokens/sec), Eff denotes power efficiency (tokens/sec/watt) and TP/Eff Impv denotes the throughput/efficiency improvement over Jetson Orin Nano. While the basic ternary FPGA design [16] is not competitive, *TerEffic* significantly outperforms the edge GPU in terms of both throughput and power efficiency, achieving **149×** throughput and **19×** power efficiency in single-batch tasks. When processing multi-batch tasks, our design exceeds the GPU’s throughput and power efficiency by **119×** and **12×**, respectively. These impressive improvements highlight the exceptional efficiency of our on-chip architecture, fully utilizing the massive on-chip bandwidth compared to the GPU’s off-chip DRAM. Moreover, while GPUs lack low-precision support, our customized TMUs unlock substantial computational capabilities through efficient ternary operations.

#### D. HBM-Assisted Architecture Evaluation

The HBM-assisted architecture is used to accelerate larger models with a single card. As discussed in Section IV-B2, the single-batch latency is 2,400 cycles/layer for the 370M model, and the throughput is thereby 4,340 tokens/s. By leveraging the **full-resource parallelism**, a maximum batch size of 15 is supported regardless of the model size, and the multi-batch

throughput is  $\approx 60,000$  tokens/s. As the HBM-assisted latency is constrained by the HBM bandwidth, the throughput will decrease to  $\frac{1}{n}$  when the model size increases by  $n\times$ .

The HBM power is estimated as  $P_{\text{HBM}} = 9.2\text{W}$ . Therefore, the overall power is  $P = P_0 + P_{\text{HBM}} = 32.7\text{W}$ . Since the resource remains unchanged for varying model sizes, the power consumption can be considered constant. We compare our results with the basic FPGA results [16] on the 1.3B model, and conduct A100 experiments on the 1.3B and 2.7B models, with the batch size set to 1 and 15 to match our design (see Section IV-B2). The results are presented in TABLE V.

TABLE V: Comparison of *TerEffic* (HBM-assisted) architecture with GPU and a basic FPGA design [16] for larger models

Model, Batch Size	Hardware	TP (tk/s)	TP Impv	Power (W)	Eff (tk/s/W)	Eff Impv
1.3B,1	FPGA [16]	24	0.05×	13.9	2	0.5×
1.3B,1	A100	499	1×	119.6	4	1×
1.3B,1	<i>TerEffic</i>	1,085	2×	32.7	33	8×
1.3B,15	A100	6,757	1×	131.6	51	1×
1.3B,15	<i>TerEffic</i>	15,000	2×	32.7	459	9×
2.7B,1	A100	250	1×	124.0	2	1×
2.7B,1	<i>TerEffic</i>	521	2×	32.7	16	8×
2.7B,15	A100	3,433	1×	138.3	25	1×
2.7B,15	<i>TerEffic</i>	7,200	2×	32.7	220	9×

Although the HBM-assisted architecture lacks the benefits of on-chip inference, our design still achieves significantly higher efficiency than GPUs by leveraging the advantages of ternary LLMs. For multi-batch tasks, where GPUs typically excel, our design is enhanced by the **full-resource parallelism** and continues to deliver superior performance. While the A100 can handle a massive batch size, a batch size of 15 is sufficient for typical edge tasks, where throughput with smaller batch sizes becomes more critical.

#### E. Further Estimations on 7B Model

Based on the previous results, we estimate the performance on a 7B model, which is a commonly used LLM size. Our HBM-assisted design is estimated to deliver a single-batch throughput of  $\approx 200$  tokens/sec with a power consumption of 33W, comparable to the typical power usage of a personal laptop. In comparison, FlightLLM [29], one of the state-of-the-art FPGA LLM accelerators, achieved a throughput of 55 tokens/sec for a 7B model on the same U280 FPGA by leveraging sparsity. Apple’s newly launched M4 Max, which is specifically optimized for local AI deployment, is estimated to achieve 100 tokens/sec in inference for an 8B model [40]. Given that our FPGA is based on the 16nm process while the Apple M4 Max uses the 3nm process, our HBM-assisted design can achieve 10× better power efficiency projected on the same technology node. With larger on-chip memory and further development of model compression techniques, our on-chip architecture has the potential to deliver even greater performance. Other high-performance LLM accelerators, such as Cerebras [41] and Groq [42], have also benefited from on-chip inference and achieved remarkable throughput of several thousand tokens per second [43]. However, these chips utilize massive on-chip SRAM (e.g., 44GB for Cerebras WSE-3

engine [44]) and consume substantial energy as high as several kilowatts, which confines their use to data centers rather than edge environments.

## VI. CONCLUSION

We have introduced *TerEffic*, an FPGA-based accelerator designed to enable efficient on-chip LLM inference by leveraging the benefits of ternary quantization. Our key innovations — 1.6-bit weight compression, specialized TMUs, and compute-memory alignment — enable unprecedented efficiency for edge deployment while preserving accuracy. The fully on-chip architecture excels at processing smaller models, while the HBM-assisted variant extends support to larger models with strong performance. Our work establishes a foundation for future research in hardware-efficient LLM deployment, particularly in resource-constrained environments where power efficiency is paramount.

## REFERENCES

- [1] OpenAI, “Chatgpt (mar 14 version) [large language model],” 2023. [Online]. Available: <https://chat.openai.com/chat>
- [2] Anthropic, “Claude: A large language model,” 2023. [Online]. Available: <https://www.anthropic.com/>
- [3] Google, “Google gemini,” 2024, version [insert version number here] [Large language model]. [Online]. Available: <https://cloud.google.com/gemini/docs/discover/works>
- [4] G. Hinton, J. Dean, and O. Vinyals, “Distilling the knowledge in a neural network,” 03 2014, pp. 1–9.
- [5] M. AI, “Llama 3.2: Connect 2024 vision for edge and mobile devices,” 2024, accessed: 2024-11-18. [Online]. Available: <https://ai.meta.com/blog/llama-3-2-connect-2024-vision-edge-mobile-devices/>
- [6] OpenAI, “Gpt-4o mini: Advancing cost-efficient intelligence,” 2024, accessed: [insert access date here]. [Online]. Available: <https://openai.com/index/gpt-4o-mini-advancing-cost-efficient-intelligence/>
- [7] TechCrunch, “Openai unveils gpt-4o mini, a small ai model powering chatgpt,” July 2024, accessed: 2024-11-18. [Online]. Available: <https://techcrunch.com/2024/07/18/openai-unveils-gpt-4o-mini-a-small-ai-model-powering-chatgpt/?guccounter=1>
- [8] A. Gholami, Z. Yao, S. Kim, C. Hooper, M. Mahoney, and K. Keutzer, “Ai and memory wall,” *IEEE Micro*, vol. PP, pp. 1–5, 05 2024.
- [9] J. Lin, J. Tang, H. Tang, S. Yang, W.-M. Chen, W.-C. Wang, G. Xiao, X. Dang, C. Gan, and S. Han, “Awq: Activation-aware weight quantization for on-device llm compression and acceleration,” *Proceedings of Machine Learning and Systems*, vol. 6, pp. 87–100, 2024.
- [10] A. Tseng, J. Chee, Q. Sun, V. Kuleshov, and C. De Sa, “Quip#: Even better llm quantization with hadamard incoherence and lattice codebooks,” *arXiv preprint arXiv:2402.04396*, 2024.
- [11] S. Aggarwal, H. J. Damsgaard, A. Pappalardo, G. Franco, T. B. Preuser, M. Blott, and T. Mitra, “Shedding the Bits: Pushing the Boundaries of Quantization with Minifloats on FPGAs,” in *2024 34th International Conference on Field-Programmable Logic and Applications (FPL)*. Los Alamitos, CA, USA: IEEE Computer Society, Sep. 2024, pp. 297–303.
- [12] X. Hu, Y. Chen, D. Yang, S. Zhou, Z. Yuan, J. Yu, and C. Xu, “I-llm: Efficient integer-only inference for fully-quantized low-bit large language models,” *arXiv preprint arXiv:2405.17849*, 2024.
- [13] H. Bai, W. Zhang, L. Hou, L. Shang, J. Jin, X. Jiang, Q. Liu, M. Lyu, and I. King, “Binarybert: Pushing the limit of bert quantization,” 01 2021, pp. 4334–4348.
- [14] H. Wang, S. Ma, L. Dong, S. Huang, H. Wang, L. Ma, F. Yang, R. Wang, Y. Wu, and F. Wei, “Bitnet: Scaling 1-bit transformers for large language models,” *arXiv preprint arXiv:2310.11453*, 2023.
- [15] S. Ma, H. Wang, L. Ma, L. Wang, W. Wang, S. Huang, L. Dong, R. Wang, J. Xue, and F. Wei, “The era of 1-bit llms: All large language models are in 1.58 bits,” *arXiv preprint arXiv:2402.17764*, 2024.
- [16] R.-J. Zhu, Y. Zhang, E. Siferman, T. Sheaves, Y. Wang, D. Richmond, P. Zhou, and J. K. Eshraghian, “Scalable matmul-free language modeling,” *arXiv preprint arXiv:2406.02528*, 2024.
- [17] Z. Yuan, R. Zhou, H. Wang, L. He, Y. Ye, and L. Sun, “Vit-1.58 b: Mobile vision transformers in the 1-bit era,” *arXiv preprint arXiv:2406.18051*, 2024.
- [18] M. Daliri, Z. Song, and C. Yang, “Unlocking the theory behind scaling 1-bit neural networks,” 2024. [Online]. Available: <https://arxiv.org/abs/2411.01663>
- [19] I. Hubara, M. Courbariaux, D. Soudry, R. El-Yaniv, and Y. Bengio, “Binarized neural networks,” *NIPS*, vol. 29, 2016.
- [20] M. Rastegari, V. Ordonez, J. Redmon, and A. Farhadi, “Xnor-net: Imagenet classification using binary convolutional neural networks,” in *European conference on computer vision*. Springer, 2016, pp. 525–542.
- [21] F. Li, B. Liu, X. Wang, B. Zhang, and J. Yan, “Ternary weight networks,” 2022. [Online]. Available: <https://arxiv.org/abs/1605.04711>
- [22] H. You, Y. Guo, Y. Fu, W. Zhou, H. Shi, X. Zhang, S. Kundu, A. Yazdanbakhsh, and Y. Lin, “Shiftaddllm: Accelerating pretrained llms via post-training multiplication-less reparameterization,” *arXiv preprint arXiv:2406.05981*, 2024.
- [23] B. Li, S. Pandey, H. Fang, Y. Lyu, J. Li, J. Chen, M. Xie, L. Wan, H. Liu, and C. Ding, “FTRANS: Energy-efficient acceleration of transformers using FPGA,” [Online]. Available: <http://arxiv.org/abs/2007.08563>

[24] H. Khan, A. Khan, Z. Khan, L. B. Huang, K. Wang, and L. He, "NPE: An FPGA-based overlay processor for natural language processing." [Online]. Available: <http://arxiv.org/abs/2104.06535>

[25] Y. Han and Q. Liu, "HPTA: A high performance transformer accelerator based on FPGA," in *2023 33rd International Conference on Field-Programmable Logic and Applications (FPL)*, pp. 27–33, ISSN: 1946-1488. [Online]. Available: <https://ieeexplore.ieee.org/document/10296316/>?arnumber=10296316

[26] S. Hong, S. Moon, J. Kim, S. Lee, M. Kim, D. Lee, and J.-Y. Kim, "DFX: A low-latency multi-FPGA appliance for accelerating transformer-based text generation," in *2022 55th IEEE/ACM International Symposium on Microarchitecture (MICRO)*, pp. 616–630. [Online]. Available: <https://ieeexplore.ieee.org/document/9923883/>?arnumber=9923883

[27] H. Peng, S. Huang, S. Chen, B. Li, T. Geng, A. Li, W. Jiang, W. Wen, J. Bi, H. Liu, and C. Ding, "A length adaptive algorithm-hardware co-design of transformer on fpga through sparse attention and dynamic pipelining," in *Proceedings of the 59th ACM/IEEE Design Automation Conference*, ser. DAC '22, vol. 33. ACM, Jul. 2022, p. 1135–1140. [Online]. Available: <http://dx.doi.org/10.1145/3489517.3530585>

[28] H. Chen, J. Zhang, Y. Du, S. Xiang, Z. Yue, N. Zhang, Y. Cai, and Z. Zhang, "Understanding the potential of FPGA-based spatial acceleration for large language model inference." [Online]. Available: <http://arxiv.org/abs/2312.15159>

[29] S. Zeng, J. Liu, G. Dai, X. Yang, T. Fu, H. Wang, W. Ma, H. Sun, S. Li, Z. Huang *et al.*, "Flightllm: Efficient large language model inference with a complete mapping flow on fpgas," in *Proceedings of the 2024 ACM/SIGDA International Symposium on Field Programmable Gate Arrays*, 2024, pp. 223–234.

[30] M. Huang, A. Shen, K. Li, P. Haoxiang, B. Li, and H. Yu, "EdgeLLM: A highly efficient CPU-FPGA heterogeneous edge accelerator for large language models." [Online]. Available: <http://arxiv.org/abs/2407.21325>

[31] O. Muller, A. Prost-Boucle, A. Bourge, and F. Pétrot, "Efficient decompression of binary encoded balanced ternary sequences," *IEEE Transactions on Very Large Scale Integration (VLSI) Systems*, vol. 27, no. 8, pp. 1962–1966, 2019.

[32] G. Ilharco, C. Ilharco, I. Turc, T. Dettmers, F. Ferreira, and K. Lee, "High performance natural language processing," in *Proceedings of the 2020 Conference on Empirical Methods in Natural Language Processing: Tutorial Abstracts*, A. Villavicencio and B. Van Durme, Eds. Online: Association for Computational Linguistics, Nov. 2020, pp. 24–27.

[33] Z. Qin, S. Yang, and Y. Zhong, "Hierarchically gated recurrent neural network for sequence modeling," *Advances in Neural Information Processing Systems*, vol. 36, 2024.

[34] Y. Dauphin, A. Fan, M. Auli, and D. Grangier, "Language modeling with gated convolutional networks," 12 2016.

[35] A. Vaswani *et al.*, "Attention is all you need," vol. 30, 2017.

[36] T. Hugo *et al.*, "Llama: Open and efficient foundation language models," 2023. [Online]. Available: <https://arxiv.org/abs/2302.13971>

[37] Z. Li, Y. Zhang, B. Sui, Z. Xing, and Q. Wang, "Fpga implementation for the sigmoid with piecewise linear fitting method based on curvature analysis," *Electronics*, vol. 11, no. 9, 2022. [Online]. Available: <https://www.mdpi.com/2079-9292/11/9/1365>

[38] B. Zhang and R. Sennrich, "Root mean square layer normalization," 12 2019.

[39] NVIDIA, "Tensorrt," <https://developer.nvidia.com/tensorrt>, accessed: Date.

[40] S. Vosler, "The 200b parameter cruncher macbook pro: Exploring the m4 max llm performance," 2024, accessed: 2024-11-18. [Online]. Available: <https://seanvosler.medium.com/the-200b-parameter-cruncher-macbook-pro-exploring-the-m4-max-llm-performance-8fd571a94783>

[41] Cerebras, "Introducing cerebras inference: Ai at instant speed," *Cerebras AI*, 2024. [Online]. Available: <https://cerebras.ai/blog/introducing-cerebras-inference-ai-at-instant-speed>

[42] Groq, "12 hours later, groq is running llama 3 instruct 8b & 70b by meta ai on its lpu inference engine," 2023, accessed: 2024-11-18. [Online]. Available: <https://groq.com/12-hours-later-groq-is-running-llama-3-instruct-8-70b-by-meta-ai-on-its-lpu-inference-engine/>

[43] K. Freund, "Cerebras now the fastest llm inference processor—it's not even close," *Forbes*, November 2024. [Online]. Available: <https://www.forbes.com/sites/karlfreund/2024/11/18/cerebras-now-the-fastest-llm-inference-processor-its-not-even-close/>

[44] Cerebras, "Cerebras product system," <https://cerebras.ai/product-system/>, 2024, accessed: 2024-11-15.